IEEE Access
Multidisciplinary | Rapid Review | Open Access Journal

Received October 7, 2020, accepted October 20, 2020, date of publication October 29, 2020, date of current version November 11, 2020.

Digital Object Identifier 10.1109/ACCESS.2020.3034691

Extended Gate Field Effect Transistor Based Sensor for Detection of Trace Amounts of Anti-Depressant Drug

SHOKOOFEH SHEIBANI[1,2], ADRIAN M. IONESCU[2], (Fellow, IEEE), AND PARVIZ NOROUZI[1]
[1]Center of Excellence in Electrochemistry, Department of Chemistry, University of Tehran, Tehran 1417466191, Iran
[2]Nanolab, Ecole Polytechnique Fédérale de Lausanne, 1015 Lausanne, Switzerland

Corresponding author: Parviz Norouzi (pnorouzi@ut.ac.ir)

This works was supported in part by the Research Council of University of Tehran, and in part by the Internal Grant of Nanolab, Ecole Polytechnique Fédérale de Lausanne.

ABSTRACT Citalopram hydrobromide (CP) is a selective serotonin reuptake inhibitor for the treatment of the depressive disorder. In this work, a novel label-free recognition method based on an extended gate field-effect transistor (EGFET) for selective determination of CP is investigated. A Pt electrode covered by a modified PVC membrane, as the sensing part, is connected to the gate of a MOSFET transducer. Two types of PVC membranes containing ion-pairs, CP ion and tetraphenylborate or phosphotungstate ions (with different percentages), are used in this study. The obtained results indicate that the PVC membrane containing 7 % CP-tetraphenylborate has the highest sensitivity, with a detection limit of 10^{-12} M. The sensor exhibits two linear response ranges, in the ranges of $10^{-11}-10^{-7}$ M and $10^{-6}-10^{-2}$ M, characterized by different sensitivities. The proposed method shows clear advantages in terms of increased accuracy, sensitivity, precision, and selectivity. The sensor is successfully applied to assay citalopram in tablets. The features of simplicity in preparation, fast response, capability for the miniaturization, and easy operatory, make the sensor a promising candidate for future integrated lab-on-chip devices for pharmaceutical quality control measurements.

INDEX TERMS Citalopram, ion selective field-effect transistor, extended gate field-effect transistor, PVC.

I. INTRODUCTION

Detection and quantification of drugs in pharmaceutical products and biological samples has attracted considerable research interest. This is due to the development of selective and effective drugs, and for the realization of their therapeutic and toxic effects [1], [2]. 1-(3-dimethylaminopropyl)-1-(4-fluorophenyl)-5-phthalan carbonitrile or in short Citalopram (CP), Fig. 1, has been widely used for the treatment of depression, a major disorder affecting human health in today's society. CP is a member of drug group known as selective serotonin reuptake inhibitors (SSRIs), which have been become very popular depression treatment [3]. Moreover, CP has been prescribed for the treatment of panic disorder, obsessive-compulsive disorder and social anxiety disorder [4]. The CP level, in pharmaceutical combinations and some real samples, has been measured by the exploitation of thin-layer liquid chromatography (HPTLC) [5], gas chromatography mass spectrometry GC/GC–MS [6], capillary electrophoresis [7], liquid chromatography tandem mass spectrometry (LC–MS/MS) [8], liquid chromatography–electrospray ionization mass spectrometry [9] and nuclear magnetic resonance spectrometric NMR methods [10]. These methods have many disadvantages such as high cost, long measurement process, and the requirement of tedious sample

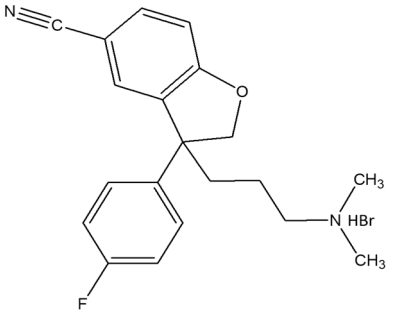

FIGURE 1. Chemical structure of CP.

The associate editor coordinating the review of this manuscript and approving it for publication was Wuliang Yin.

pretreatment. Additionally, chromatography methods require the use of large amounts of highly purified solvents, which are often hazardous and lead to the production of toxic laboratory waste. Therefore, devising a new analysis method with high sensitivity, simplicity, and efficiency for the detection of this drug is an essential. These features besides short response time and high selectivity can be offered by electrochemical methods. [11], [12].

Until now, numerous electrochemical sensors, including potentiometric and voltammetric sensors, have been introduced for selective detection of CP in different samples [13]–[20]. Potentiometric sensors work based on the Ion-Selective Electrodes (ISEs), which mostly employ symmetric or asymmetric PVC membrane containing insoluble ion-pair of the drug cation as the sensing components. Although these potentiometric sensors have shown wide dynamic range, they are not able to achieve low detection limit. Voltammetric sensors are based on the redox reaction of the CP on the surface of different electrode materials. Although, the detection limit of these sensors is in the range of nanomolar, the dynamic range is limited to 3 and even 1 decay of the CP concentration. Therefore, the design of a new sensor, with a low detection limit along with a wide dynamic range, is an open scientific and technological challenge. In recent years, among electrochemical sensors, Ion Sensitive Field Effect Transistors (ISFETs) have attracted much attention due to the ability of low cost, miniaturization, low power operation, and co-integrated read-outs [21]–[23]. ISFET technology is a subset of potentiometric sensors, with this advantage that is not affected by signal distortions arising from the environment, as the input gate potential is connected immediately to the electrical FET transducer [24]. They are capable of converting very low values of the electrical charge (e.g. in the vicinity of the transistor gate) such as any species carrying charge (similarly to ions), to a detectable electrical signal which is the variation of the FET drain current. The fundamental operation of an ISFET sensor is similar to a Metal-Oxide-Semiconductor Field Effect Transistors (MOSFETs), in which the threshold voltage of the device depends on the metal gate work function. However, in an ISFET, the threshold voltage is modulated by the charge of an ion sensitive membrane existing on top of the gate [24]. Although ISFETs have high charge sensitivity, chemical reactions between the gate dielectric and different species existing in the solution may result in the change of gate stack characteristics. Therefore, the electrical characteristic of an ISFET sensor can deteriorate and drift over time. To overcome this issue, Extended-Gate (EG) FETs have been proposed for sensing applications [25], [26]. In this configuration, the base transducer is a standard MOSFET, while the sensing element is formed by depositing a specific sensing layer on the extension of the metal gate that can be an external electrode, electrically connected to the MOSFET gate.

The EGFET configuration has shown significant advantages due to the separation of the insulated transducing element from the sensing layer. Higher stability, low drift, and low temperature sensitivity have been reported for the sensors based on this device [26]. Moreover, the EGFET configuration enables us to easily dispose of the damaged gate without substitution of the main transducer MOSFET.

This work presents a new analysis technique by means of an EGFET for the detection of trace amounts of CP in a wide dynamic range of CP concentrations. The EG is an easily prepared platinum electrode covered with a selective PVC membrane containing insoluble ion pair of CP cation as the sensing element. The comparative application of two different ion pairs (with different portions in the PVC membrane) were investigated, to optimize the suitable membrane composition to reach the lowest detection limit in a wide dynamic range. Characterizations of the sensor were examined and the selectivity of the sensor was validated. The sensor was successfully applied for the measurement of CP in its pharmaceutical formulation.

II. EXPERIMENTAL DETAILS

A. CHEMICALS AND MATERIALS

All materials and reagents were of analytical grades and at the highest available purity. High-molecular weight polyvinylchloride (PVC) was purchased from Fluka. The chloride salts of the necessary cations, sodium tetrahydrofuran (THF), dibutyl phthalate (DBP), and sodium tetraphenyl borate (NaTPB) were purchased from Sigma-Aldrich. Sodium phosphotungstate (NaPT) was obtained from Merck. CP hydrobromide standard powder was supplied by the local pharmacy Temad (Tehran, Iran). All solutions were prepared by deionized (DI) water.

Sputtered Pt electrodes on glass substrate were purchased from MicruX Technologies. Each chip has a central circle printed Pt electrode with a thickness of 150 nm and the diameter of 1 mm.

B. STANDARD CP SOLUTIONS

The stock standard solution of CP (0.1 M) was prepared in DI water (pH: 6.2). Other working standard solutions were prepared through the dilution of the stock solution with DI water to give solutions in the concentration range of 10^{-13} to 10^{-2} M. The solutions were protected from light and stored in a refrigerator at 4 °C.

C. PREPARATION OF THE CP TABLET SAMPLES

Ten tablets of pharmaceutical CP, containing 20 mg of CP/tablet (tablets were purchased from Sobhan Daru and Kimia Daru), were weighed, and the average weight of one tablet was calculated. Then, the tablets were crushed and finely powdered, and the average weight of one tablet was dissolved in DI water, and then the solution was filtered through filter paper into a 100 mL volumetric flask. Then the volume was brought up to the mark with the DI water.

D. SYNTHESIS OF THE ION-PAIRS

Two kinds of the ion-pairs complex, which are used in the PVC membrane of the sensors, were prepared by mixing gradually the solutions of CP (30 mg in 2 mL DI water) and a solution of one of the suitable organic salt with hydrophobic large anions of NaTPB or NaPT (30 mg in 4 mL DI water). The resulting precipitates (CPTPB and CPPT) were filtered and rinsed with DI water and then dried at room temperature for 24 hours.

E. FABRICATION OF THE SENSING EXTENDED GATE ELECTRODE COVERED WITH SENSITIVE MEMBRANE

The proposed sensor structure consists of two parts: the MOSFET transducer and a sensing extended gate electrode. The extended gate of the proposed EGFET sensor is a circle-shape Pt electrode covered by a sensitive PVC membrane. To prepare the PVC membrane, certain weights of the ion-pair (CPPT or CPTPB) compound, the plasticizer (DPB), and ionic additive (NaTPB) with the total weight of 0.1 gr were mixed uniformly in 1.0 mL of fresh THF. Then, the sample was placed on a heater at 50 °C temperature for 45 min for the evaporation of the THF, and hence an oily mixture was formed. Afterward, 2 μL of the mixture was cast on the surface of the Pt electrode by means of a micropipette. The electrode was kept at room temperature for at least 12 h to be dried. Finally, for conditioning, the electrode was soaked in the solution of CP with the concentration of 10^{-3} M for about 24 h. Five kinds of sensors with five different PVC membranes were fabricated: sensors I, II, III, IV, and V, have 5 %wt CPPT, 7 %wt CPPT, 5 %wt CPTPB, 7 %wt CPTPB and 10 %wt CPTPB respectively, while for all the sensors, the ratio of 20 %wt PVC and 2 %wt NaTPB was used.

F. STRUCTURE OF THE EGFET SENSOR AND MEASUREMENT METHOD

The chip containing a modified Pt electrode was placed on the base of a static cell (purchased from MicruX Technologies). The modified electrode was connected via a metallic pin and wire to the gate of the commercial n-channel MOSFET (MOSFET of the ALD1106 IC), which was placed on a printed circuit board (PCB). In fact, the MOSFET serves as the electrical transducer of the fabricated sensor. The source and drain connections were designed on the PCB to be connected to the ports of the semiconductor parameter analyzer. When the cap of the microcell is placed on top of the chip, an open static cell with a volume of the 400 μl is formed, which was filled with the measurement solution. The gate voltage was applied to an Ag/AgCl reference electrode placed in the measurement solution of the static cell. All measurements took place in an electrical shielding box to prevent any light exposure or electromagnetic interference. The schematic view of the setup is depicted in Fig. 2. For recording the response of the sensor, the static cell was filled with 350 μL of the standard solution of the CP with known concentration. Then, to reach equilibrium in each concentration, the electrode was left for 1.5 min. Finally, the response of the sensor was recorded as the I_{DS}-V_{ref} characteristic of the MOSFET by the semiconductor parameter analyzer.

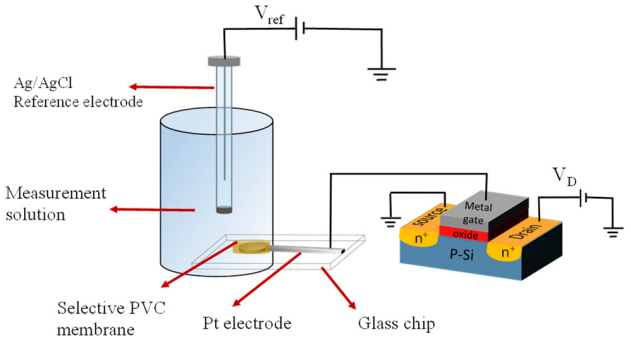

FIGURE 2. Schematic of the experimental setup based on the EGFET sensor with selective PVC membrane on Pt electrode, measurement solution, and reference electrode.

G. APPARATUS

Fourier transform infrared (FT-IR) analysis for the membrane films was performed using Nicolet 6700 FT-IR from Thermo Scientific. The X-ray diffraction (XRD) analysis of the membranes was carried out by Bruker D8 Discover XRD system, using the following operating conditions: CuK α sealed tube operated at 40 kV and 40mA, measured from 5 to 70° 2θ at 0.01 step with $\lambda = 0.154056$ nm. The prepared membranes were also characterized using Field emission scanning electron microscopy (FESEM) and Energy dispersive X-ray (EDX) spectroscopy using Zeiss Merlin EDX equipped with FE-SEM. The characterizations of the proposed EGFET sensor were investigated by the semiconductor parameter analyzer HP 4155B.

III. RESULTS AND DICUSSION

A. MEMBRANE CHARACTERIZATION

FT-IR technique was used to identify the composition of the synthesized membranes. Figs 3a and 3b indicate the FT-IR spectra of the membranes of the sensor I and sensor III, respectively, in comparison with the membrane matrix without any ion-pairs. As can be seen, the C–Cl stretching mode and CH_2 deformation peaks, which are expected to be at 834 and 1332 cm^{-1} in the PVC, are shifted to 840 and 1324 cm^{-1} in the PVC–DBP system, respectively [27]. Furthermore, molecular interaction between PVC and DBP leads to a type of H bonding between the C = O of the DBP and the H attached to the same carbon as the chloride of PVC. This interaction is verified by the shift in C–H rocking mode which is expected to be at 1,255 cm^{-1} in the PVC but is shifted to 1274 cm^{-1} in the PVC–DBP system [27]. Additionally, the peak at 1720 cm^{-1} is related to the carbonyl stretching vibration in the ester group of DBP [28]. The spectra of the membrane of the sensors I and III are mainly similar to the spectrum of the membrane matrix. However, there are some

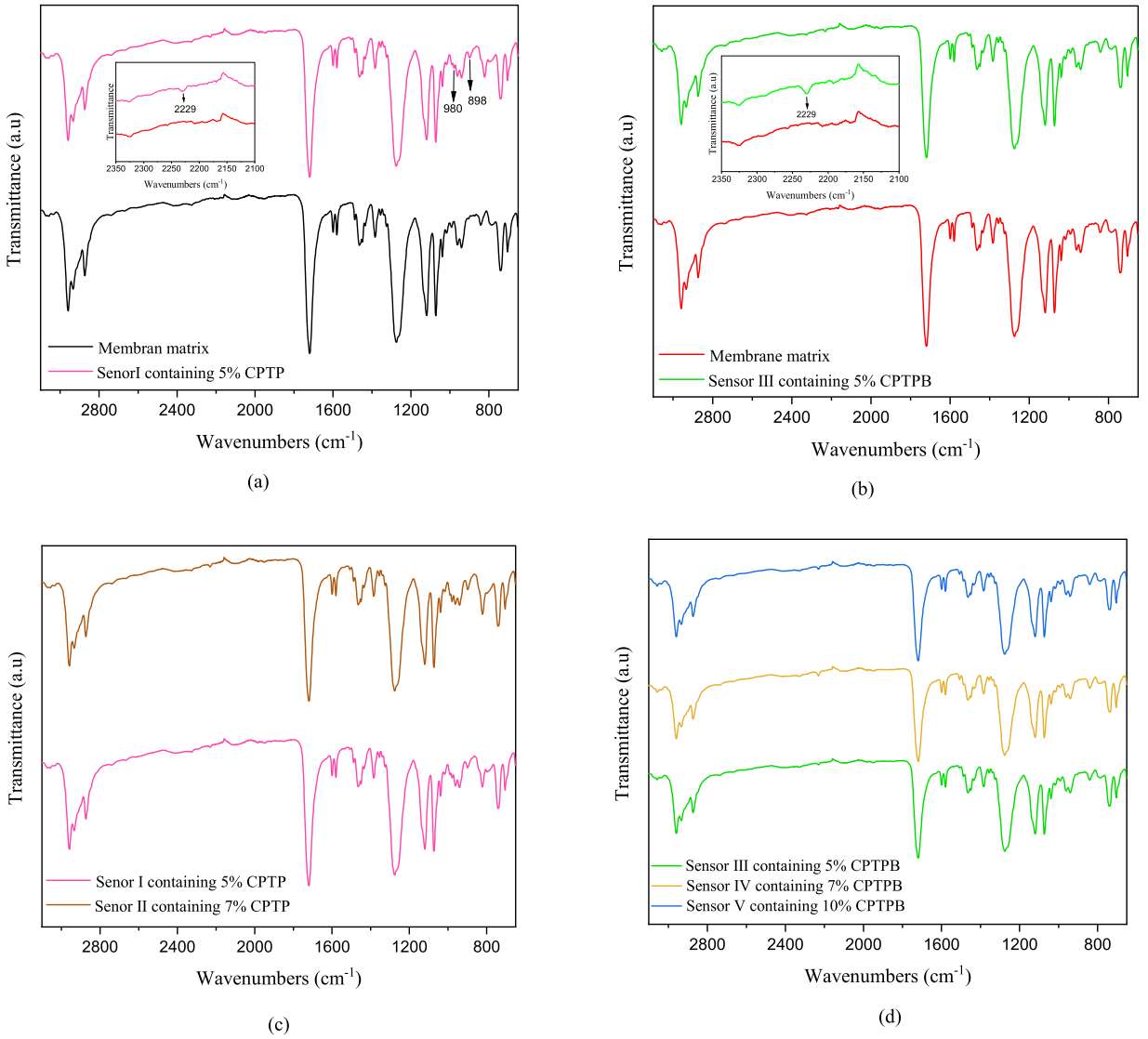

FIGURE 3. FT-IR spectra of the different sensor membranes containing different percentages of one of the two types of ion-pairs (CPPT or CPTPB) in the membrane composition. (a) membrane of the sensor I in comparison with the matrix of the membrane containing no ion-pair (b) membrane of the sensor III in comparison with the matrix of the membrane containing no ion-pair (c) membrane of the sensor I in comparison with the membrane of the sensor II (d) membrane of the sensor III in comparison with the membranes of the sensors IV and V.

different peaks related to the existence of the ion-pairs. The peak located at 2229 cm^{-1} in the membranes spectra is the signal of–C≡N existing in the CP cation. Moreover, the presence of the PT ions in the membrane composition of the sensor I is confirmed by the appearance of two characteristics bands: a peak at 980 cm^{-1} assigned to the vibrational modes of ν_{ac} P–O and ν_{ac} W–O_t, and a peak at 898 cm^{-1} related to the vibrational modes of ν_{ac} W–O_{2c1}–W and ν_{ac} W–O_{2c2}–W [29]. Additionally, it is evident from Figs. 3c and 3d that there is no shift of the peaks because of the enhancement of the ion-pairs percentage from 5% to 7% or 10% in the membrane compositions.

In addition to FT-IR analysis, the membranes of the sensors were analyzed using XRD technique to investigate the crystallinity of their structure. The results are depicted in Fig. 4. All five kinds of membranes revealed an amorphous morphology. However, the sensors with the same type of ion-pair have the same pattern in XRD spectra. The membranes containing CPTPB ion-pair have slightly higher intensity compared to the membranes containing CPPT. This means that the degree of amorphousness in the membrane structure was decreased by adding CPTPB to the membrane composition. This effect is supported by increasing the intensity of the spectra as the CPTPB percentage was enhanced in the membrane composition.

The surface morphology of the proposed extended gate electrodes was characterized by FESEM coupled with EDX for elemental analysis. Fig. 5 compares the SEM images of the sensors II and IV containing 7% CPPT and 7% CPTPB, with the SEM image of the membrane containing no ion-pairs. The surfaces of all the membranes have no defect, although there are white spots in the SEM images of the

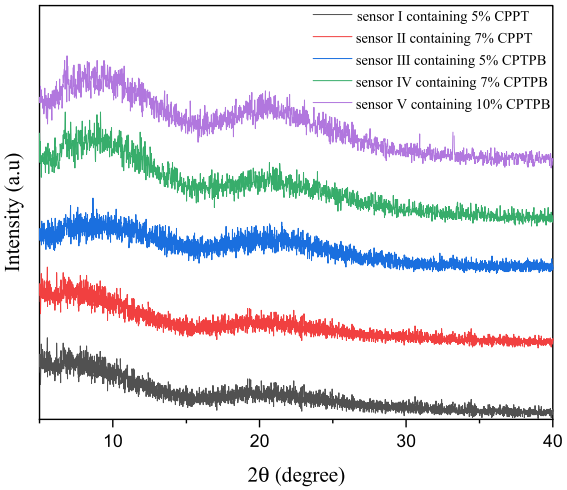

FIGURE 4. XRD spectra of the sensor membranes containing different percentages of one of the two types of ion-pairs (CPPT or CPTPB) in the membrane composition.

sensors II and IV (Figs. 5b and 5c). These spots are distributed almost homogeneously and are referred to ion-pairs, which cause the sensitivity of the sensors towards CP cations [30]. However, the surface of the sensor II seems rougher than the one of sensor IV. This effect is in accordance with XRD investigation, where sensor IV has a higher intensity than to sensor II.

The elemental composition of the membranes of the sensors II and IV was confirmed by the EDX examination. The resultant spectra are depicted next to the related SEM image of each sensor. Both membranes show the peaks of Cl and O related to the existence of PVC and DBP, respectively. Additionally, the peaks of F and N confirm the presence of the CP in the membrane composition. However, the EDX spectrum of sensor II shows the peak of W due to the existence of the PT ions in the membrane composition. Moreover, the membrane of the sensor II has a higher O ratio due to the existence of O in the PT ions, while the membrane of the sensor IV has a higher ratio of C as the result of the presence of C in TPB ions.

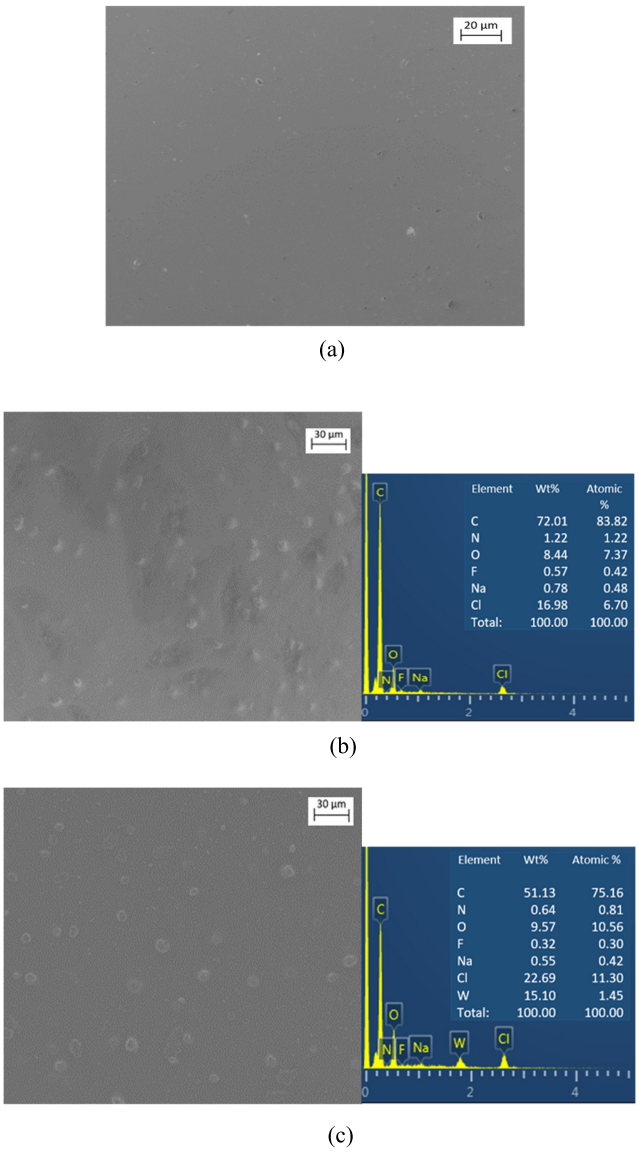

FIGURE 5. (a) SEM image of the membrane matrix without any ion-pairs (b) SEM image and related EDX spectrum of the sensor II containing 7% of CPTP ion-pair (c) SEM image and related EDX spectrum of the sensor IV containing 7% of CPTPB ion-pair.

B. CP DETECTION

Selective absorption of the CP cations on the surface of the sensor is based on the ion exchange reaction of the insoluble ion-pairs in the matrix of membrane.

The ion-pairs exchange the CP cations with their TPB or TP onions [31]. However, other components of the membrane play important roles in the sensing of the target analyte. The plasticizer of the membrane is DBP, which is reported to have the best operation in extraction of hydrophobic CP cations in comparison to other plasticizers due to lower dielectric constant (equal to 6.4) of DPB. In addition, DPB prompts homogenous dissolution and diffusion mobility of the ion-pairs in the membrane [20]. Moreover, for reducing the ohmic resistance of the membrane, NaTPB (as the ionic additive) was used in the membrane composition. The ionic additive was used in relatively small amounts so that it does not interfere with the ion- exchange phenomena.

Fig. 6 reports the transfer characteristic of the EGFET sensors for different concentrations of CP. The drain is biased with a low voltage (100mV) to operate the transistor works in its linear region. When the EGFET based sensor is operated in the linear region and for $V_G > V_{T(EGFET)}$, the drain-source current (I_{DS}) can be analytically expressed by a simple MOSFET equation as follows [32], [33]:

$$I_{DS} = \mu_n C_{ox} \frac{W}{L} \left[\left(V_{ref} - V_{T(EGFET)} \right) V_{DS} - \frac{1}{2} V_{DS}^2 \right] \quad (1)$$

where μ_n is the carrier mobility in the channel, C_{ox} indicates the oxide capacitance per unit area, W/L represents the channel width to length ratio, V_{ref} indicates the applied potential

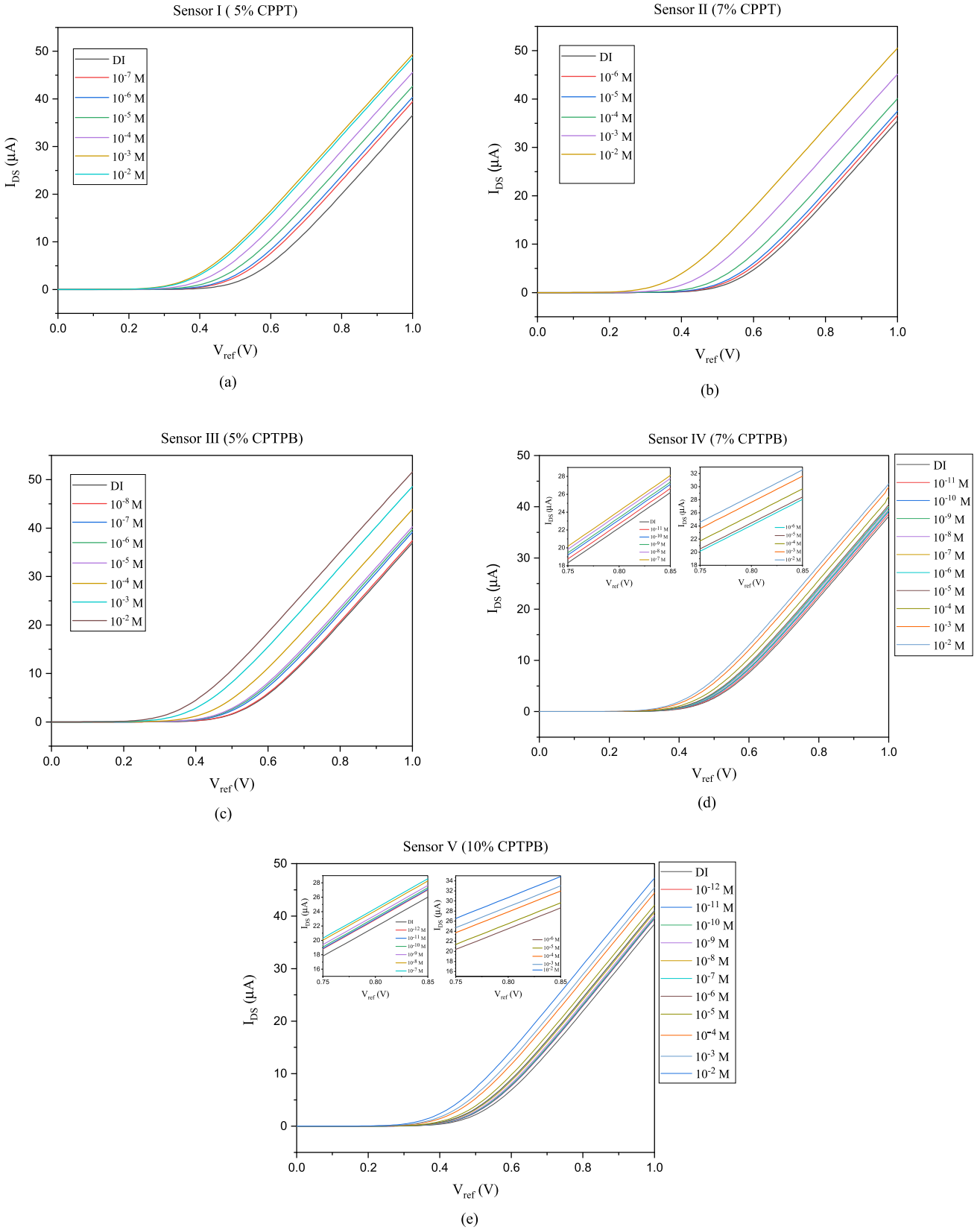

FIGURE 6. Response of the different sensors towards the CP concentrations (a) sensor I containing 5% CPPT, (b) sensor II containing 7% CPPT, (c) sensor III containing 5% CPTPB, (d) sensor IV containing 7% CPTPB, (e) sensor V containing 10% CPTPB.

TABLE 1. Optimization of the membrane ingredients.

Sensor No	*Ion pair*	*Detection limit (M)*	*Linear range (M)*	*Sensitivity (μA/decade)*	*R^2 %*	*Intercept (μA)*
I	5% CPPT	10^{-7}	10^{-6}-10^{-3}	2.55	99	41.6
II	7% CPPT	10^{-6}	10^{-5}-10^{-2}	4.47	98	42.4
III	5% CPTPB	10^{-9}	10^{-8}-10^{-6}	1.24	95	30.8
			10^{-5}-10^{-2}	3.92	99.5	43.2
IV	7% CPTPB	10^{-12}	10^{-11}-10^{-7}	0.3	97.3	26.19
			10^{-6}-10^{-2}	1.23	97.2	31.1
V	10% CPTPB	10^{-13}	10^{-12}-10^{-7}	0.31	93	26.5
			10^{-6}-10^{-2}	1.58	98	31.2

to the reference electrode in order to bias the extended gate of the MOSFET in the measurement solution, and V_{DS} is the drain to source voltage. $V_{T(EGFET)}$ represents the value of the threshold voltage of the EGFET, which is given by the following equation [32], [34]:

$$V_{T(EGFET)} = V_{T(MOSFET)} - \frac{\phi_M}{q} + E_{ref} + \chi^{Sol} - \psi \quad (2)$$

where $V_{T(MOSFET)}$ is the threshold voltage of a MOSFET device, ϕ_M is the work function of the metal gate electrode, E_{ref} is the potential of reference electrode, χ^{sol} is the surface dipole potential of the solvent, and ψ is the surface potential at the electrolyte and sensing membrane interface. Via parameter ψ, information from the chemical domain is transduced to the electrical domain.

The I_{DS}-V_{ref} plots were obtained by sweeping the voltage of the reference electrode from 0.0 to 1.0 V, while the V_{DS} was set at a constant value of 0.1 V in order to make the transistor work at the linear region. In all the subfigures of Fig. 6, the first black line is related to the response of each sensor in DI water containing no CP, and the red line is the first shifted line related to the lowest concentration of the CP, which makes a left shift in the I_{DS}-V_{ref} curve respect to the response of the sensor to DI water. As can be seen in Fig. 6, all the five sensors show a left shift in the I_{DS}-V_{ref} curves of the sensor by increasing the CP concentration. In other words, at a known applied potential respect to the reference electrode, the current value of I_{DS} enhances with the increase of the CP concentration. This is attributed to the membrane ability to absorb CP cations by equilibrium. The absorbed CP cations on the sensing electrode reduces the threshold voltage of the EGFET and cause a left shift in the transfer characteristic of the EGFET sensor. Therefore, by increasing the CP concentration in the measurement solution, the number of absorbed CP cations to the membrane increase and the I_{DS}-V_{ref} curve shifts more to the left direction.

In order to reach to the lowest detection limit, the composition of the sensing membrane was optimized. In this direction, two types of ion-pairs (CPTPB and CPPT) with different percentages in the PVC membrane were tested (sensors: I-IV) [20], [31]. The tested membranes have different structures according to the XRD and SEM analysis. Additionally, the number and the type of ion-pairs directly affect the membrane capability to attract CP cations, which change the threshold voltage of the EGFET sensor by modulating the parameter ψ in equation 2. Therefore, for the same concentrations of the CP, the responses of the proposed sensors containing different membranes are different.

On the base of previous explanations, for plotting the response of the sensors against the CP concentration in a calibration curve, the value of I_{DS} at the constant potential of $V_{ref} = 0.8$ V (higher than the threshold voltage, $V_{T(EGFET)}$) was extracted from the I_{DS}-V_{ref} curve related to each concentration of the analyte. The results of this plotting for all five kinds of sensors are depicted in the Table. 1. As can be seen, the sensors constructed with the membrane containing CPPT show lower sensitivity towards the detection of CP compared to the sensors constructed with the membrane containing CPTPB. At optimum values of the two types of ion-pairs in the membrane composition, the sensor II having 5% CPPT shows the detection limit of 10^{-7} M. However, the detection limit for the sensor IV with 7% CPTPB is as low as 10^{-12} M.

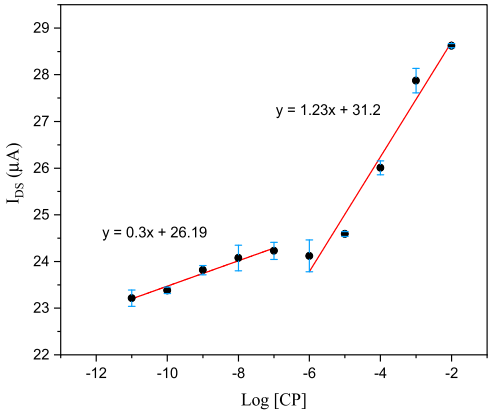

FIGURE 7. Calibration curve of the sensor IV with optimized membrane composition containing 7% CPTPB ion-pair.

Also, sensor IV appears to have two quasi-linear response regions of the drain current, I_{DS}, versus the log [CP], (Fig. 7). These two regions are characterized by different sensitivities: one is related to the low concentrations up to the 10^{-7}M

TABLE 2. Comparison of the features of the proposed sensor with previously reported CP electrochemical sensors.

Sensor type	*Detection limit (M)*	*Linear range (M)*	*Sensitivity*	*Reference*
potentiometric	1.25×10^{-7}	2.5×10^{-7}-10^{-3}	50.77(mV/decade)	[13]
potentiometric	7.0×10^{-8}	10^{-7}-10^{-3}	57.3 (mV/decade)	[20]
voltammetric	2.5×10^{-8}	10^{-7}-10^{-6}	0.58 (μA/decade)	[14]
voltammetric	5×10^{-9}	1.2×10^{-8}-1.54×10^{-6}	35.7 (μA/decade)	[15]
voltammetric	4.9×10^{-8}	5×10^{-7}-5×10^{-5}	1.1662 (μA/decade)	[1]
voltammetric	4.4×10^{-8}	9×10^{-8}-10^{-6}	2.7497 (μA/decade)	
		10^{-6}-11×10^{-6}	0.2564 (μA/decade)	[17]
		11×10^{-6}-10^{-4}	0.0572 (μA/decade)	
In this work	10^{-12}	10^{-11}-10^{-7}	0.3 (μA/decade)	
		10^{-6}-10^{-2}	1.23 (μA/decade)	

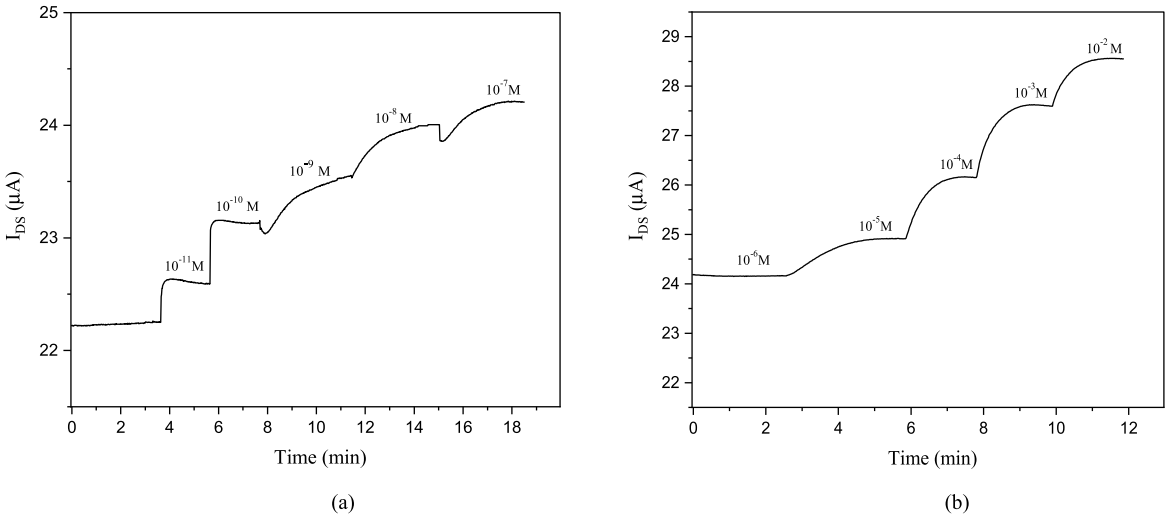

FIGURE 8. Dynamic response of the sensor IV (with optimized membrane composition) through the real time measurement for different concentrations of CP in (a) low concentrations of CP and (b) high concentrations of CP.

of CP, and the other is related to high concentrations up to the 10^{-2}M of CP. Although increasing the CPTPB ion-pair percentage from 7% to 10% produces higher level of current, it reduces the sensor precision in low concentrations of CP. Therefore, sensor IV, which has 7% of the CPTPB ion-pair in the membrane composition, was selected as the sensor with optimum composition. The related calibration curve of this sensor is depicted in Fig. 7, with the mean amount of three replicate measurements for each concentration. In addition, this sensor is compared with the recent reported electrochemical sensors introduced for the detection of CP in Table. 2. The proposed sensor of this work shows clear advantages in terms of detection limit and linear range.

C. DYNAMIC RESPONSE OF THE SENSOR THROUGH THE REAL TIME MEASUREMENT

In order to investigate the response of the sensor through the time, the offset potential of the gate was fixed at 0.8 V (the same as the potential used to extract I_{DS} from I_{DS}-V_{ref} curves); also, the drain to source voltage was set at 0.1 V (like previous measurements). Then the value of the drain current, I_{DS} (response of the sensor) versus time was recorded, when the analyte concentration was increased step by step. As can be seen in Fig. 8, the static response time was less than 30 s for 10^{-11} M and 10^{-10}M of CP. This sharp response of the sensor at low concentrations could be attributed to the existence of a large number of empty sites on the sensor membrane. However, at higher concentrations between 10^{-9} M and 10^{-7} M, the response time average increased to about 2 min. The increase of the response time in higher concentrations could be related to kinetic factors in adsorption and reduction in the available adsorption sites on the surface of the sensor. Moreover, at concentrations higher than 10^{-6} M, the behavior or sensitivity of the sensor and sensor response interred in its second linear range.

D. VALIDATION OF THE METHOD

1) SELECTIVITY

One of the most important characteristic of any sensor device is its selectivity, which describes the specificity of the sensor towards the target in the presence of interfering compounds. Practically, for examining the sensor selectivity, it was exposed to the different solutions containing 10^{-11} M CP and various concentrations of the interfering species. The measurements were performed based on recorded I_{DS}-V_{ref} curves, where the response of the sensor as I_{DS} at V_{ref} of 0.8 V was measured for all the concentrations of the interfering species. Then, a normalization in the response was done, and the parameter S was defined. Where $I_{DS(sp)}$ is the response of the sensor in the solution containing a known concentration of interfering species, and $I_{DS(CP)}$ is the response of the sensor in the solution containing just 10^{-11} M CP. The results of this normalization were plotted against the concentrations and depicted in Fig. 9. The tested species, did not affect the response of the sensor significantly even in their high concentration, which is 10^9 times higher than the concentration of the CP existing in the solution.

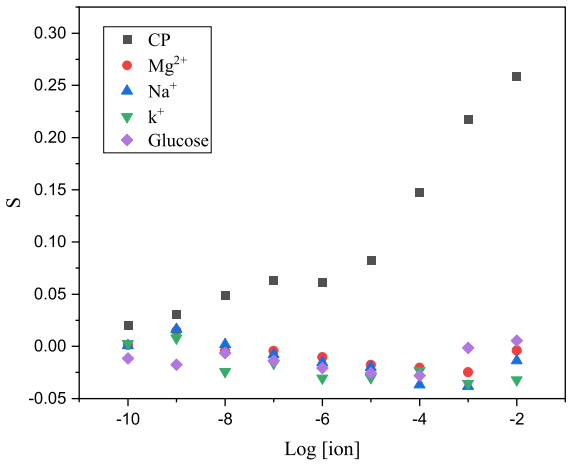

FIGURE 9. Response of the sensor IV towards CP in comparison to other interfering cations and glucose.

2) PRECISION

In order to obtain precision of the technique, repeatability and reproducibility were investigated. For the repeatability monitoring, five replicate standard samples with the concentrations of 0.24 μg/mL, and 0.24 mg/mL were measured. The mean concentrations were found to be 0.232 μg/mL and 0.245 mg/mL with respective RSD values of 2.3 and 4.5 %. Regarding the inter-day precision for validation of the reproducibility, the three concentrations of 0.024 μg/mL, 0.24 μg/mL and 0.24 mg/mL were measured for three consecutive days with three sensors, providing mean CP concentrations of 0.22 μg/mL, 0.25 μg/mL and 0.25 mg/mL and associated RSD values of 9.6, 9.3, and 5 %, respectively.

3) ACCURACY

To assess the accuracy, the values of relevant error percentage and the recovery were calculated for the mentioned concentrations. The error percentages were 4.5 and 3.7 %, and the recoveries were 95.5 and 104 %, respectively.

E. APPLICATION OF THE SENSOR TO PHARMACEUTICAL FORMULATION

For testing CP in the pharmaceutical formulation, the stoke solution of CP tablets was prepared as described in part 2.3. Measurement of the tablet solutions were done by standard addition method [35], and the signal of the sensor was measured as described in part III.B. The results of the measurements are shown in Table. 3.

TABLE 3. The results of the measured CP tablets.

Applied sample	*Labeled amount (mg/tab)*	*Found (mg/tab)*	*RSD*	*Recovery %*
Sobhan Daru	20	19	2.3	95
Kimia Daru	20	19.2	3	96

IV. CONCLUSION

In this study, we demonstrated and validated by experiments a successful design of an EGFET sensor for selective recognition of the CP drug. The unique characteristic of this sensor, in comparison to previous reported electrochemical devices, is the ability of the sensor to detect trace concentrations of the CP with a fast response time. The dynamic linear range of the sensor response is wide enough to cover both low concentrations and high concentrations of the CP. Additionally, the measurement with the proposed sensor is easy and effective to put in practice. Moreover, the extended gate configuration of this FET sensor, with external electrodes enables a quick replacement of the sensitive surface of the sensor while maintaining the same readout device. This feature is notably important for healthcare or quality control devices, as the sensitivity of the sensor can be retained by using fresh sensitive surface for each new test. Overall, the proposed EGFET provides many advantages, which make it an excellent candidate to be employed in quality control of the pharmaceutical industry. Additionally, due to miniaturized EGFET and electrode, the proposed sensing structure is suited for integrated lab-on-chip devices.

ACKNOWLEDGMENT

Authors are thankful to Dr. Ali Saeidi and Dr. Junrui Zhang for their kind help and support in this research.

REFERENCES

[1] L. Daneshvar, G. H. Rounaghi, Z. Es'haghi, M. Chamsaz, and S. Tarahomi, "Fabrication a new modified electrochemical sensor based on au–Pd bimetallic nanoparticle decorated graphene for citalopram determination," *Mater. Sci. Eng., C*, vol. 69, pp. 653–660, Dec. 2016, doi: 10.1016/j.msec.2016.07.025.

[2] Q. H. Meng and D. Gauthier, "Simultaneous analysis of citalopram and desmethylcitalopram by liquid chromatography with fluorescence detection after solid-phase extraction," *Clin. Biochem.*, vol. 38, no. 3, pp. 282–285, Mar. 2005, doi: 10.1016/j.clinbiochem.2004.12.009.

[3] R. J. Milne and K. L. Goa, "Citalopram: A review of its pharmacodynamic and pharmacokinetic properties, and therapeutic potential in depressive illness," *Drugs*, vol. 41, no. 3, pp. 450–477, Mar. 1991, doi: 10.2165/00003495-199141030-00008.

[4] M. Pirdadeh-Beiranvand, A. Afkhami, and T. Madrakian, "Cloud point-magnetic dispersive solid phase extraction for the spectrofluorometric determination of citalopram," *J. Mol. Liquids*, vol. 241, pp. 43–48, Sep. 2017, doi: 10.1016/j.molliq.2017.05.139.

[5] N. Dhavale, S. Gandhi, S. Sabnis, and K. Bothara, "Simultaneous HPTLC determination of escitalopram oxalate and clonazepam in combined tablets," *Chromatographia*, vol. 67, nos. 5–6, pp. 487–490, Mar. 2008, doi: 10.1365/s10337-008-0524-7.

[6] H. H. Maurer and J. Bickeboeller-Friedrich, "Screening procedure for detection of antidepressants of the selective serotonin reuptake inhibitor type and their metabolites in urine as part of a modified systematic toxicological analysis procedure using gas chromatography-mass Spectrometry*," *J. Anal. Toxicol.*, vol. 24, no. 5, pp. 340–347, Jul. 2000, doi: 10.1093/jat/24.5.340.

[7] J. J. Berzas-Nevado, M. J. Villaseñor-LLerena, C. Guiberteau-Cabanillas, and V. Rodríguez-Robledo, "Enantiomeric screening of racemic citalopram and metabolites in human urine by entangled polymer solution capillary electrophoresis: An innovatory robustness/ruggedness study," *Electrophoresis*, vol. 27, no. 4, pp. 905–917, Feb. 2006, doi: 10.1002/elps.200500413.

[8] E. Weisskopf, A. Panchaud, K. A. Nguyen, D. Grosjean, J.-M. Hascoát, C. Csajka, C. B. Eap, and N. Ansermot, "Stereoselective determination of citalopram and desmethylcitalopram in human plasma and breast milk by liquid chromatography tandem mass spectrometry," *J. Pharmaceutical Biomed. Anal.*, vol. 131, pp. 233–245, Nov. 2016, doi: 10.1016/j.jpba.2016.08.014.

[9] E. Weisskopf, A. Panchaud, K. A. Nguyen, D. Grosjean, J.-M. Hascoát, C. Csajka, C. B. Eap, and N. Ansermot, "Simultaneous determination of selective serotonin reuptake inhibitors and their main metabolites in human breast milk by liquid chromatography-electrospray mass spectrometry," *J. Chromatography B*, vol. 1057, pp. 101–109, Jul. 2017, doi: 10.1016/j.jchromb.2017.04.039.

[10] S. M. Ali and S. Shamim, "Quantitative ROESY analysis of computational models: Structural studies of citalopram and β-cyclodextrin complexes by 1 H-NMR and computational methods," *Magn. Reson. Chem.*, vol. 53, no. 7, pp. 526–535, Jul. 2015, doi: 10.1002/mrc.4250.

[11] S. Jeong, J. Park, D. Pathania, C. M. Castro, R. Weissleder, and H. Lee, "Integrated magneto–electrochemical sensor for exosome analysis," *ACS Nano*, vol. 10, no. 2, pp. 1802–1809, Feb. 2016, doi: 10.1021/acsnano.5b07584.

[12] G. Maduraiveeran, M. Sasidharan, and V. Ganesan, "Electrochemical sensor and biosensor platforms based on advanced nanomaterials for biological and biomedical applications," *Biosensors Bioelectron.*, vol. 103, pp. 113–129, Apr. 2018, doi: 10.1016/j.bios.2017.12.031.

[13] R. Gutiérrez-Climente, A. Gómez-Caballero, N. Unceta, M. A. Goicolea, and R. J. Barrio, "A new potentiometric sensor based on chiral imprinted nanoparticles for the discrimination of the enantiomers of the antidepressant citalopram," *Electrochimica Acta*, vol. 196, pp. 496–504, Apr. 2016, doi: 10.1016/j.electacta.2016.03.010.

[14] A. Izadyar, D. R. Arachchige, H. Cornwell, and J. C. Hershberger, "Ion transfer stripping voltammetry for the detection of nanomolar levels of fluoxetine, citalopram, and sertraline in tap and river water samples," *Sens. Actuators B, Chem.*, vol. 223, pp. 226–233, Feb. 2016, doi: 10.1016/j.snb.2015.09.048.

[15] H. Ghaedi, A. Afkhami, T. Madrakian, and F. Soltani-Felehgari, "Construction of novel sensitive electrochemical sensor for electro-oxidation and determination of citalopram based on zinc oxide nanoparticles and multi-walled carbon nanotubes," *Mater. Sci. Eng., C*, vol. 59, pp. 847–854, Feb. 2016, doi: 10.1016/j.msec.2015.10.088.

[16] P. Norouzi, P. Daneshgar, M. R. Ganjali, and A. Moosavi-Movahedi, "Novel method for determination of trace amounts of citalopram in tablets by fast Fourier continuous cyclic voltammetry at au microelectrode in flowing solutions," *J. Brazilian Chem. Soc.*, vol. 18, no. 1, pp. 231–238, 2007, doi: 10.1590/S0103-50532007000100027.

[17] M.-B. Gholivand and A. Akbari, "A novel voltammetric sensor for citalopram based on multiwall carbon nanotube/(poly(p-aminobenzene sulfonic acid)/β-cyclodextrin) ," *Mater. Sci. Eng., C*, vol. 62, pp. 480–488, May 2016, doi: 10.1016/j.msec.2016.01.066.

[18] H. Keypour, S. G. Saremi, H. Veisi, and M. Noroozi, "Electrochemical determination of citalopram on new schiff base functionalized magnetic fe 3 o 4 nanoparticle/MWCNTs modified glassy carbon electrode," *J. Electroanal. Chem.*, vol. 780, pp. 160–168, Nov. 2016, doi: 10.1016/j.jelechem.2016.08.022.

[19] T. A. Ali, G. G. Mohamed, A. M. Al-Sabagh, and M. A. Migahed, "A New Screen-printed Ion Selective Electrode for Determination of Citalopram Hydrobromide in Pharmaceutical Formulation," *Chin. J. Anal. Chem.*, vol. 42, no. 4, pp. 565–572, Apr. 2014, doi: 10.1016/S1872-2040(13)60725-2.

[20] M. R. Ganjali and B. Larijani, "All-solid-state citalopram sensor and its application for the analysis of pharmaceutical formulations," *Anal. Bioanal. Electrochem.*, vol. 7, no. 5, pp. 635–646, 2015.

[21] S. Kalra, M. J. Kumar, and A. Dhawan, "Dielectric-modulated field effect transistors for DNA detection: Impact of DNA orientation," *IEEE Electron Device Lett.*, vol. 37, no. 11, pp. 1485–1488, Nov. 2016, doi: 10.1109/LED.2016.2613110.

[22] Y. Rayanasukha, S. Pratontep, S. Porntheeraphat, W. Bunjongpru, and J. Nukeaw, "Non-enzymatic urea sensor using molecularly imprinted polymers surface modified based-on ion-sensitive field effect transistor (ISFET)," *Surf. Coatings Technol.*, vol. 306, pp. 147–150, Nov. 2016, doi: 10.1016/j.surfcoat.2016.05.060.

[23] J. Zeng, L. Kuang, N. Miscourides, and P. Georgiou, "A 128×128 current-mode ultra-high frame rate ISFET array with in-pixel calibration for real-time ion imaging," *IEEE Trans. Biomed. Circuits Syst.*, vol. 14, no. 2, pp. 359–372, Apr. 2020, doi: 10.1109/TBCAS.2020.2973508.

[24] P. Grändler and J. Janata, "Chemical sensors: An introduction for scientists and engineers," *Phys. Today*, vol. 61, p. 56, Dec. 2008, doi: 10.1063/1.2897955.

[25] A. M. Khalifa, S. A. Abdulateef, E. A. Kabaa, N. M. Ahmed, and F. A. Sabah, "Study of acidosis, neutral and alkalosis media effects on the behaviour of activated carbon threads decorated by zinc oxide using extended gate FET for glucose sensor application," *Mater. Sci. Semicond. Process.*, vol. 108, Mar. 2020, Art. no. 104911, doi: 10.1016/j.mssp.2019.104911.

[26] Z. Iskierko, M. Sosnowska, P. S. Sharma, T. Benincori, F. D'Souza, I. Kaminska, K. Fronc, and K. Noworyta, "Extended-gate field-effect transistor (EG-FET) with molecularly imprinted polymer (MIP) film for selective inosine determination," *Biosens. Bioelectron.*, vol. 74, pp. 526–533, Dec. 2015, doi: 10.1016/j.bios.2015.06.073.

[27] S. Ramesh and L. J. Yi, "FTIR spectra of plasticized high molecular weight PVC–LiCF3SO3 electrolytes," *Ionics*, vol. 15, no. 4, pp. 413–420, Aug. 2009, doi: 10.1007/s11581-008-0279-z.

[28] A. Abdolmaleki, S. Mallakpour, and F. Azimi, "Microwave and ultrasound-assisted synthesis of poly(vinyl chloride)/riboflavin modified MWCNTs: Examination of thermal, mechanical and morphology properties," *Ultrason. Sonochem.*, vol. 41, pp. 27–36, Mar. 2018, doi: 10.1016/j.ultsonch.2017.09.018.

[29] A. J. Bridgeman, "Density functional study of the vibrational frequencies of β-Keggin heteropolyanions," *Chem. Phys.*, vol. 287, no. 1, pp. 55–69, Feb. 2003, doi: 10.1016/S0301-0104(02)00978-3.

[30] H. E. Kormal, A. Demirel Özel, S. Sayän, M. Yälmaz, and E. Käç, "Development of a pH sensing membrane electrode based on a new calix[4]arene derivative," *Talanta*, vol. 132, pp. 669–675, Jan. 2015, doi: 10.1016/j.talanta.2014.10.032.

[31] M. Nebsen, C. M. El-Maraghy, and H. Salem, "Ion selective membrane electrodes for determination of citalopram hydrobromide in drug product and in presence of its degradation products," *Int. J. Process.*, vol. 7, no. 4, p. 14, 2015.

[32] S. Pullano, C. Critello, I. Mahbub, N. Tasneem, S. Shamsir, S. Islam, M. Greco, and A. Fiorillo, "EGFET-based sensors for bioanalytical applications: A review," *Sensors*, vol. 18, no. 11, p. 4042, Nov. 2018, doi: 10.3390/s18114042.

[33] S. A. Pullano, "Design and fabrication of an EGFET based chemical sensor using transistor association technique," in *Proc. IEEE Int. Symp. Med. Meas. Appl. (MeMeA)*, Jun. 2020, pp. 1–5, doi: 10.1109/MeMeA49120.2020.9137280.

[34] A. K. Mishra, D. K. Jarwal, B. Mukherjee, A. Kumar, S. Ratan, and S. Jit, "CuO nanowire-based extended-gate field-effect-transistor (FET) for pH sensing and enzyme-free/receptor-free glucose sensing applications," *IEEE Sensors J.*, vol. 20, no. 9, pp. 5039–5047, May 2020, doi: 10.1109/JSEN.2020.2966585.

[35] R. Chokkareddy, N. Thondavada, N. K. Bhajanthri, and G. G. Redhi, "An amino functionalized magnetite nanoparticle and ionic liquid based electrochemical sensor for the detection of acetaminophen," *Anal. Methods*, vol. 11, no. 48, pp. 6204–6212, Dec. 2019, doi: 10.1039/C9AY01743G.

SHOKOOFEH SHEIBANI received the B.S. degree in chemistry and the M.S. degree in analytical chemistry from the University of Tehran, Tehran, Iran, in 2012 and 2014, respectively, where she is currently pursuing the Ph.D. degree in electrochemistry.

Since 2019, she has been a Research Assistant and a Ph.D. Exchange Student with the Nanolab, Ecole Polytechnique Fédérale de Lausanne, Switzerland. Her research interests include design of electrochemical and field effect transistor-based sensors and biosensors.

ADRIAN M. IONESCU (Fellow, IEEE) received the B.S./M.S. degree from the Polytechnic Institute of Bucharest, Romania, in 1989, and the Ph.D. degree from the National Polytechnic Institute of Grenoble, France, in 1997.

He held staff and/or visiting positions with LETI-CEA, Grenoble, France, Grenoble INP, France, and Stanford University, USA, from 1998 to 1999. He was a Visiting Professor with the Tokyo Institute of Technology in 2016. He is currently a Professor with the Swiss Federal Institute of Technology, Lausanne, Switzerland. He has published more than 600 articles in international journals and conferences.

Dr. Ionescu has been a member of the Swiss Academy of Technical Sciences (SATW) since 2015. He served on the IEDM and VLSI conference technical committees. He received the Annual Award of the Technical Section from the Romanian Academy of Sciences, in 1994, and the Blondel Medal for contributions to the progress in engineering sciences in the domain of electronics in 2009. He was a 2013 recipient of the IBM Faculty Award in engineering. He also served as the General Chair for the ESSDERC-ESSCIRC Conference in 2016.

PARVIZ NOROUZI received the B.Sc. degree in analytical chemistry, Iran, and the Ph.D. degree in electrochemistry from the College of Arts and Science, University of Saskatchewan, Canada. He is currently a Professor of electrochemistry with the College of science, University of Tehran, Iran. He has been authored/coauthored over 550 articles and eight book chapters. He has given tutorials in many universities. His current research interests include instrument development in electrochemistry, sensor/biosensor design, interfacing with computer/smart phone, adaptation of development of heath monitoring devices on smart phone/over a networks, and the IoT-based systems for monitoring of compounds in liquid and gas. He received many awards, such as the Distinguished Professor Award, the Outstanding Researcher Award, and the Outstanding Research Project Award from the University of Tehran and the Tehran University of Medical Sciences. He served as a reviewer and a guest editor for many international journals.